Eur. Phys. J. C 31, 343–349 (2003)
Digital Object Identifier (DOI) 10.1140/epjc/s2003-01381-3

THE EUROPEAN PHYSICAL JOURNAL C

On the investigation of the proton structure using QED Compton events in ep scattering

V. Lendermann[1,a], H.-C. Schultz-Coulon[2], D. Wegener[2]

[1] Deutsches Elektronen-Synchrotron (DESY), 22607 Hamburg, Germany
[2] Institut für Physik, Universität Dortmund, 44221 Dortmund, Germany

Received: 11 July 2003 /
Published online: 30 October 2003 –

Abstract. QED Compton scattering at HERA is discussed in terms of the information it may reveal on the proton structure at low momentum transfers Q^2. Detailed Monte Carlo studies are performed which show that the analysis of inelastic QED Compton events allows the extension of present HERA structure function measurements to a kinematic domain, which up to now was only accessed in fixed target data. For these studies an improved version of the COMPTON event generator is used, where special emphasis has been put on modelling the hadronic final state at low invariant masses.
As the low Q^2 regime is sometimes also discussed in the context of the collinear approximation and the possibility of measuring the photonic content of the proton, the Monte Carlo studies are also used to check the validity of this approach. It is found that the proposed concept of a photon density γ of the proton does not provide sufficient accuracy for the description of inelastic QED Compton scattering.

1 Introduction

Measurements of deep-inelastic lepton-proton scattering (DIS) provide information that is crucial to our understanding of proton structure. Since the fixed target experiments have discovered scaling violations [1, 2], much progress has been made in extending the kinematic region covered in terms of the Bjorken variable x and the four-momentum transfer squared, Q^2. This holds especially for the ep scattering experiments at HERA which, with their wealth of data, have shown that the Q^2 evolution of the proton structure function $F_2(x, Q^2)$ is well described by perturbative Quantum Chromodynamics (pQCD) throughout a wide range in x and Q^2 [3–6]. However, at small Q^2 deviations from pQCD predictions are observed [7,8], indicating the transition into a regime where non-perturbative effects dominate and the data can only be described by phenomenological models such as those derived from the Regge approach [9].

In order to study this non-perturbative regime, the structure function F_2 has been measured at very low values of Q^2 and x, which are accessible at HERA via special devices mounted close to the outgoing electron beam [8] thus facilitating measurements of the scattered electron at very low angles. These devices, however, do not cover the transition region at $Q^2 \sim 1\,\mathrm{GeV}^2$, which up to now has only been investigated using "shifted vertex" [7, 10] and Initial State Radiation [11, 12] data. In this paper the possibility to extend the kinematic domain of HERA into this region using QED Compton (QEDC) events, i.e. ep events with wide angle hard photon radiation, is discussed.

The present studies are based on a modified version [13] of the COMPTON event generator [14] which in particular comprises several dedicated software packages for a complete description of the low mass hadronic final state. Apart from studying the potential of QEDC events to access the low Q^2 region this new version of the COMPTON program thus also allows investigating the possibility to measure in the fixed target region at higher x, because the result of such a measurement crucially depends on the accurate description of the hadronic final state at low masses.

The possibility to measure the proton structure function F_2 at low Q^2 using QEDC events was first discussed by Blümlein et al. [15,16]. In the framework of the equivalent photon approximation the authors introduced the concept of a photon density of the proton[1], γ, to be valid at very low virtualities Q^2. This function has been computed by de Rújula and Vogelsang [17] when proposing an extraction method for γ from HERA QEDC data. The validity of this approach is discussed in the second part of the paper, where it is shown that the collinear approximation does not provide a sufficient description of inelastic QEDC scattering and that measurements of the QEDC cross section with reasonable precision can thus not be interpreted in terms of the photon density function.

[a] *Corresponding author.* E-mail: victor@mail.desy.de

[1] Sometimes also denoted as $f_{\gamma|p}$ or $D_{\gamma|p}$

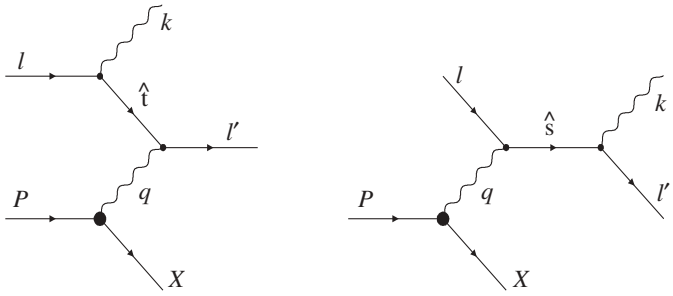

Fig. 1. Lowest order Feynman diagrams for the radiative process $ep \to e\gamma X$ with photon emission from the electron line. l, P represent the four-momenta of the incoming electron and the incoming proton, while l', k and X are the momenta of the scattered electron, the radiated photon and the hadronic final state, respectively. $\hat{s}$ and $\hat{t}$ denote the squared four-momenta of the virtual lepton

2 QEDC Monte Carlo simulation

Radiative processes in *ep* scattering, as depicted in Fig. 1, may be split into three different classes [18,19] with (i) the bremsstrahlung or Bethe-Heitler process corresponding to small masses of both the virtual electron and the virtual photon, (ii) the QED Compton process with a low virtual photon and a large virtual electron mass and finally (iii) the radiative DIS process where the photon is collinear either with the incoming (Initial State Radiation, ISR) or the outgoing (Final State Radiation, FSR) electron. All three classes correspond to distinct experimental signatures. For the QEDC scattering process the final state topology is given by an azimuthal back-to-back configuration of the outgoing electron and photon detected under rather large scattering angles. In this configuration their transverse momenta balance such that very low values of the exchanged photon virtuality Q^2 are experimentally accessible.

To correctly describe the process $ep \to e\gamma X$ the standard kinematic variables x and Q^2, used to describe inclusive deep-inelastic scattering (DIS), have to be redefined in order to account for the additional photon in the final state

$$Q^2 = -q^2 = -(l - l' - k)^2\,, \quad x = \frac{Q^2}{2P \cdot (l - l' - k)}\,. \quad (1)$$

Here l and P are the four-momenta of the incoming electron and the incoming proton, and l' and k represent the momenta of the scattered electron and the radiated photon, respectively (Fig. 1). Three further independent variables are needed for a full description of the differential QEDC scattering cross section. In the formalism presented in [18] the Lorentz invariant scale variable $x_\gamma = q{\cdot}l/P{\cdot}l$ and the scattering solid angle Ω^* defined in the centre-of-mass frame of the virtual Compton process and encapsulating two degrees of freedom are employed. The cross section is then given by [18]

$$\frac{d^4\sigma^{ep\to e\gamma X}}{dx\,dx_\gamma\,dQ^2\,d\Omega^*} = f^T_{\gamma^*/p}(x, x_\gamma, Q^2)\left[\frac{d\sigma}{d\Omega^*}\right]^T + f^L_{\gamma^*/p}(x, x_\gamma, Q^2)\left[\frac{d\sigma}{d\Omega^*}\right]^L\,, \quad (2)$$

where $[d\sigma/d\Omega^*]^{T,L}$ are the differential cross sections of the process $e\gamma^* \to e\gamma$ for transverse and longitudinal polarised photons, fully calculable in the framework of QED [18], and $f^{T,L}_{\gamma^*/p}$ represent the corresponding virtual photon spectra, which may be expressed in terms of the photo-absorption cross sections $\sigma^{T,L}_{\gamma^* p}$. Depending on the value of the invariant mass of the hadronic final state,

$$W = \sqrt{Q^2\frac{1-x}{x} + m_p^2}\,, \quad (3)$$

one has to consider three separate contributions, in order to specify $\sigma^{T,L}_{\gamma^* p}$:

1. Elastic scattering, for which the proton stays intact ($W = m_p, x = 1$). This channel is well measured, and the cross section is given by the electric and magnetic form factors G_E and G_M;
2. Resonance production, where the total mass of the hadronic final state X lies in the range $m_p + m_\pi \lesssim W \lesssim 2\,\mathrm{GeV}$;
3. Continuum inelastic scattering at $W \gtrsim 2\,\mathrm{GeV}$. In this region the $\gamma^* p$ cross section is defined through the proton structure functions F_2 and F_L.

The above cross section expression (2) is implemented in the COMPTON event generator [14]. However, as this generator was primarily written for an application in analyses of elastic QEDC events, in the original version a rather crude approach has been employed to describe the resonance region and only simple scale invariant F_2 parameterisations are used to model the continuum inelastic domain. Furthermore, no hadronisation of the final state X is performed.

As this paper aims at the investigation of inelastic QEDC events a new version of the COMPTON generator was developed [13] which includes detailed parameterisations for the resonance [20] and the continuum [21] regions. In addition, several packages for a complete simulation of the hadronic final state have been implemented into the program. For the present studies the SOPHIA package [22] is used in the range of low Q^2 or low masses, W, of the hadronic final state while the Quark Parton Model with subsequent Lund string fragmentation [23] is employed at high W and high Q^2.

3 On the measurement of F_2 using QEDC scattering

The present studies are based on a Monte Carlo sample which was generated using the new version of the COMPTON program and corresponds to an integrated luminosity of about 30 pb^{-1}; the incident beam energies used are $E_e = 27.6\,\mathrm{GeV}$ for the electron and $E_p = 820\,\mathrm{GeV}$ for the proton beam. In order to obtain a realistic simulation of the experimental conditions at the HERA *ep* detectors, the generated events were subject to the GEANT-based simulation of the H1 detector [24]. Hence, the selection criteria are adapted to the resolution and acceptance limits of the detector components relevant for this analysis.

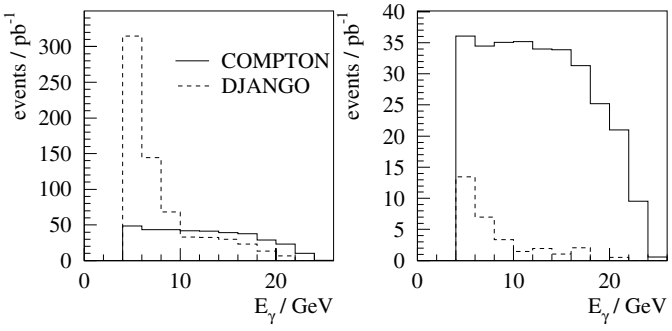

Fig. 2. Energy of the photon candidate in the backward calorimeter as calculated by the H1 simulation program. Shown are the expectations from QEDC scattering as predicted by the COMPTON generator in comparison to the DIS background simulated using DJANGO. The left and right plots show the distributions before and after applying the cut of 90° on the maximum polar angle of any further energy deposition in the calorimeters

The most important ones are the backward calorimeter[2] SpaCal [25], the liquid-argon (LAr) calorimeter and the tracking and vertex detectors [24, 26].

The analysis strategy is based on the detection of the outgoing electron and photon observed almost back-to-back in azimuth. Thus, the main experimental requirement is the existence of two electromagnetic energy depositions (clusters) with $E_\gamma, E_e > 4\,\mathrm{GeV}$ in the backward calorimeter; an additional limit is imposed on the total $e\gamma$ energy $E_e + E_\gamma > 20\,\mathrm{GeV}$ to reduce radiative corrections. In order to separate QED Compton scattering from the FSR process and still obtain inelastic QEDC events the azimuthal acoplanarity angle $A = |180° - \Delta\phi|$ is required to be below 45°, where $\Delta\phi$ represents the angle between the transverse momenta of the electron and the photon; this cut also matches a corresponding requirement in the COMPTON event generator [18]. Inelastic QEDC events are selected demanding at least one LAr cluster with energy above $E > 0.5\,\mathrm{GeV}$; as the acceptance of the LAr calorimeter is limited to $\theta \gtrsim 4°$ this cut – apart from rejecting elastic events – substantially reduces the inelastic contribution at very low masses W. After applying these criteria, background contributions from standard DIS events only appear for large angles of the hadronic final state particles where one hadron fakes a photon signal in the backward calorimeter and the current jet is observed in the backward region of the detector. This contribution is reduced by requiring no additional energy deposition apart from the two clusters to be found above $\theta_{\max} = 90°$ (see Fig. 2). Finally, only events with a reconstructed vertex are considered, in order to guarantee a correct determination of all kinematic variables. Vertices are reconstructed using the electron track detected in one of the tracking detectors, which at low y provides better resolution in z than the hadronic vertex. A brief summary of all selection criteria is given in Table 1.

[2] The z axis of the right-handed coordinate system used by H1 is defined to lie along the direction of the incident proton beam and the origin to be at the nominal *ep* interaction vertex; the backward direction is thus defined through $z < 0$

Table 1. Summary of QEDC selection criteria

Item	**Cut value**
QEDC signature	$E_\gamma, E_e > 4\,\mathrm{GeV}$
[in backward region]	$E_e + E_\gamma > 20\,\mathrm{GeV}$
	$A = \lvert 180° - \Delta\phi\rvert < 45°$
	$153° \lesssim \theta_\gamma, \theta_e \lesssim 177°$
Hadronic final state	$E > 0.5\,\mathrm{GeV}$ (within one cluster)
	$4° \lesssim \theta < 90°$
Event properties	existence of reconstructed vertex
	$\lvert z_{\mathrm{vtx}}\rvert < 30\,\mathrm{cm}$

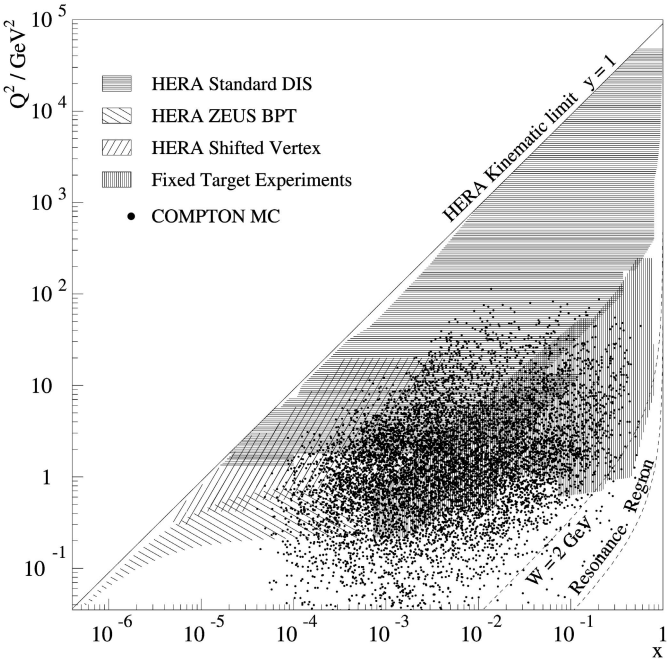

Fig. 3. Kinematic domain of continuum inelastic QED Compton events in comparison to the regions covered by inclusive DIS measurements at HERA and fixed target experiments

The phase space covered by a QEDC sample selected by the cuts described is shown in Fig. 3 for an integrated luminosity of $30\,\mathrm{pb}^{-1}$. Compared to the kinematic range accessed at HERA via standard deep-inelastic scattering, the QEDC events clearly extend to lower Q^2. For inclusive DIS the outgoing electron is not detected for such low values of Q^2 as it is scattered at small angles escaping through the beam pipe unseen. QEDC events, however, with the electron and photon in the final state balancing in transverse momentum, reach into the transition region below $Q^2 < 1.5\,\mathrm{GeV}^2$, which otherwise is only accessed through ISR [11,12] (not shown), shifted vertex [7,10] and BPT [8] data. But, these latter data do not extend the

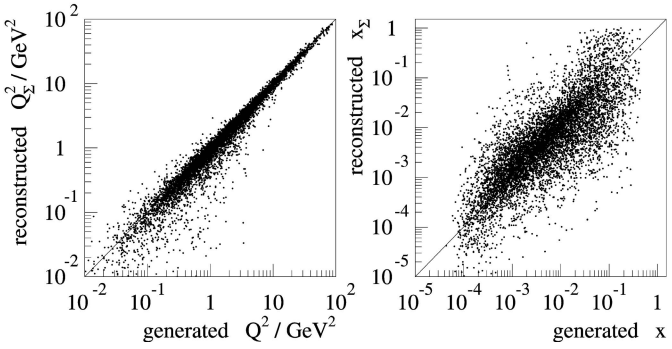

Fig. 4. Correlation between the generated and reconstructed variables Q^2 and x using the Sigma method

low Q^2 F_2 measurements to such high x as QEDC events. It is therefore the range of medium to high x which is of special interest when analysing QEDC scattering. As higher x correspond to low masses W, special emphasis had to be put into the correct modelling of the hadronic final state.

An accurate description of the hadronic final state is especially important as, for the kinematic range in question, the reconstruction of the Bjorken variable x cannot be performed using the kinematics of the outgoing electron and photon; the x resolution of this method deteriorates with $1/y = xs/Q^2$ thus becoming inapplicable at low values of the inelasticity y. For a double differential measurement of the structure function $F_2(x, Q^2)$ at $Q^2 \sim 1\,\mathrm{GeV}$ and $x \gtrsim 10^{-4}$ the variable x has thus to be reconstructed from the final state hadrons. This is done using the so-called Sigma method [27], which is based on the measurement of $\sum_i (E - p_z)_i$ summing over all objects i of the hadronic final state. To suppress the influence of calorimeter noise substantially contributing at low masses W, we use a simple approach in which only clusters with energies above the noise level of 0.5 GeV are considered when reconstructing x. Figure 4 shows the correlation between the generated and reconstructed values of Q^2 and x. It demonstrates the possibility to reconstruct the QEDC event kinematics using the hadronic final state throughout the relevant phase space region, i.e. for $0.1 \lesssim Q^2 \lesssim 10\,\mathrm{GeV}^2$ and $10^{-4} \lesssim x \lesssim 10^{-1}$. Here, the upper bound in x is given by the angular acceptance of the calorimeter, which restricts the reconstruction of the current jet in forward direction. The corresponding requirements used in this study lead to similar acceptance limitations as for the inclusive DIS measurements of H1 [4, 28] and ZEUS [5] at higher Q^2.

The expected statistical significance of an F_2 measurement based on the same COMPTON event sample with $30\,\mathrm{pb}^{-1}$ total integrated luminosity is presented in Fig. 5. In order to extract the structure function F_2 in terms of x and Q^2 the selected Monte Carlo data are divided into subsamples corresponding to a grid in x and Q^2. The bin sizes are adapted to the resolution in the measured kinematic quantities such that purity and stability in all bins shown are greater than 30%; here, the purity (stability) is defined as the ratio of the number of simulated events originating from and reconstructed in a specific bin to the number of reconstructed (generated) events in the same bin. As the proton structure function F_2 is then obtainted by a bin-by-bin unfolding method using the same Monte Carlo sample, the extracted F_2 values trivially lie on the curve representing the ALLM97 F_2 parameterisation [21] used as input to the Monte Carlo generator.

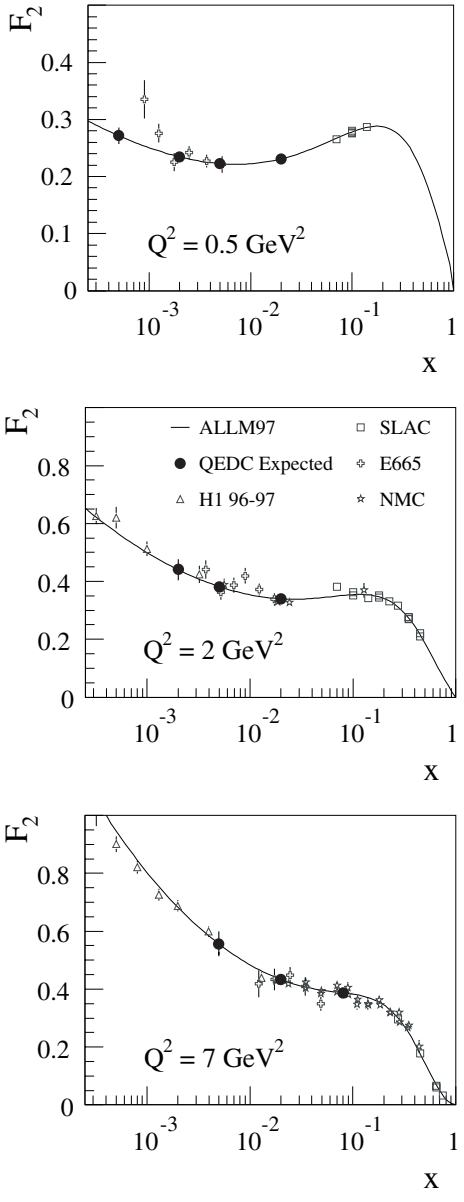

Fig. 5. Possible F_2 measurement as expected from a $30\,\mathrm{pb}^{-1}$ QEDC event sample. The expected HERA results (closed circles), estimated using the COMPTON Monte Carlo program, are shown in comparison to H1 results obtained from standard DIS data (open triangles [3]) taken during the years 1996-1997 and measurements from fixed target experiments (open squares [29], open stars [30] and open crosses [31])

Clearly, the systematic uncertainties remain to be studied in order to judge on the overall precision of the measurement. As for inclusive F_2 measurements at low y the largest error contribution is expected to come from uncertainties in the hadronic final state measurement at small

polar angles. Uncertainties specific to the QEDC Compton analysis may arise from additional background contributions and the treatment of the final state photon. They should be of smaller size.

The results demonstrate that an analysis of QEDC scattering data at HERA would add information in the low Q^2 and medium to high x region not yet covered by the HERA *ep* experiments[3]. Such an analysis would extend the present HERA measurements into the region previously covered only by fixed target data.

4 On the photon content of the proton

In contrast to the exact treatment of the QEDC scattering process, the concept of the photon content in the proton based on the collinear or equivalent photon (Weizäcker-Williams) approximation [33, 34] provides a much simpler approach to QEDC scattering and is believed to reveal basic features of photon-induced reactions involving proton beams. In this "parton model" approach the transverse component of the exchanged photon momentum is neglected and the emitted photon is assumed to be on-shell and collinear with the incident proton. This simplifies the expression for the QEDC cross section to [35]

$$\frac{d^2\sigma^{\mathrm{ep}\to\mathrm{e}\gamma\mathrm{X}}}{dx_l\, dQ_l^2} = \frac{2\pi\alpha^2}{x_l^2 s^2}\frac{1+(1-y_l)^2}{1-y_l}\,\gamma(x_l, Q_l^2)\,, \qquad (4)$$

where the "structure" function $\gamma(x_l, Q_l^2)$ parameterises the photon-parton content of the proton depending only on two degrees of freedom, the leptonic variables $Q_l^2 = -(l - l')^2$ and $x_l = \frac{Q_l^2}{2P\cdot q_l}$; at fixed centre-of-mass energy $\sqrt{s}$ the inelasticity y_l is also defined through these two variables via the relation $y_l = Q_l^2/x_l s$.

According to the above expression, an experimental determination of the double differential QED Compton scattering cross section $d^2\sigma/dx_l\, dQ_l^2$ can be interpreted as a measurement of the photon-parton density function $\gamma(x_l, Q_l^2)$. This γ function can then be applied for the computation of other *ep* and *pp* cross sections where the underlying process is mediated by a quasi-real photon exchange [36–41]. The possibility to measure the structure function $\gamma(x_l, Q_l^2)$ using QEDC events was discussed in several publications [15–17, 42]. We consider here the latest work by De Rújula and Vogelsang [17] where they proposed to compare the Q_l^2 dependence of γ at fixed x_l with its gluon counterpart $g(x, Q^2)$.

In order to judge on the feasibility of measuring γ a dedicated study of the accuracy of the collinear approximation is performed. Contrary to the prior discussion, for this study the selection criteria on energy and acoplanarity (see Table 1) are applied directly to the generated quantities. No constraints on the hadronic final state are imposed. Furthermore, following [17], it is assumed that the outgoing electron and photon can be reconstructed in the whole calorimeter acceptance. Thus, the requirements on the scattering angles are extended to $0.06 < \theta_e, \theta_\gamma < \pi - 0.06$.

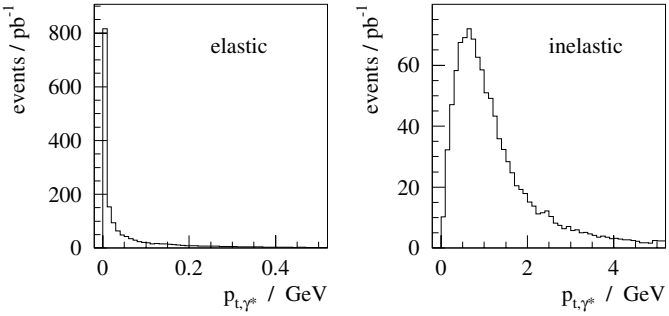

Fig. 6. Transverse momentum of the exchanged photon in elastic (left) and inelastic (right) QEDC events generated by the COMPTON program

Figure 6 shows the transverse momentum (p_{t,γ^*}) distribution of the exchanged photon in elastic and inelastic QEDC events as predicted by the COMPTON event generator. While for elastic events p_{t,γ^*} is rather small, much larger values are reached when selecting inelastic scattering processes. Thus, as in the collinear approximation one assumes p_{t,γ^*} to vanish, one can expect significant deviations when calculating event kinematics. The effect is further enhanced due to the acceptance constraints, which demand that both outgoing particles, electron and photon, are measured under finite polar angles.

A comparison between the exact calculation and the predictions from the collinear approximation is given in Fig. 7, which shows the total, i.e. the sum of the elastic and inelastic QEDC cross section as a function of Q_l^2 in bins of x_l. Significant discrepancies are observed in several bins. The exact cross sections were derived from a sample of COMPTON events generated without radiative correction. For the collinear approximation predictions have been computed analytically by Vogelsang [43] using the same set of cuts; the corresponding uncertainty of this calculation was estimated to be approximately 2%. Furthermore the elastic scattering cross sections generated by the COMPTON program and computed in the Weizsäcker-Williams approximation were compared. Very good agreement was obtained showing that the collinear approximation provides, indeed, a good description of the elastic process.

It has been checked that the difference between the F_2 parameterisations employed in the COMPTON generator and in the calculations by De Rújula and Vogelsang, cannot account for the observed discrepancies: the different predictions for γ calculated according to the relations given in [16, 17] agree within 4% [4]. The inelastic QEDC cross sections, however, deviate by up to a factor of 2 from each

[3] The kinematic domain in question could in principle also be accessed using the ZEUS BPT [8] or the H1 VLQ calorimeter [32], devices both facilitating event tagging at very low Q^2. As for the QEDC analysis it requires an accurate vertex measurement and a sufficiently good reconstruction of the hadronic final state. The same holds for Initial State Radiation events. Concerning the shifted vertex analysis, acceptance limitations at low polar angles (low y), however, restrict this method to lower values of x

[4] As the phenomenological F_2 parameterisations used in the COMPTON program have, contrary to the pQCD based PDFs employed in [17], no artificial lower Q^2 limit, we also tested

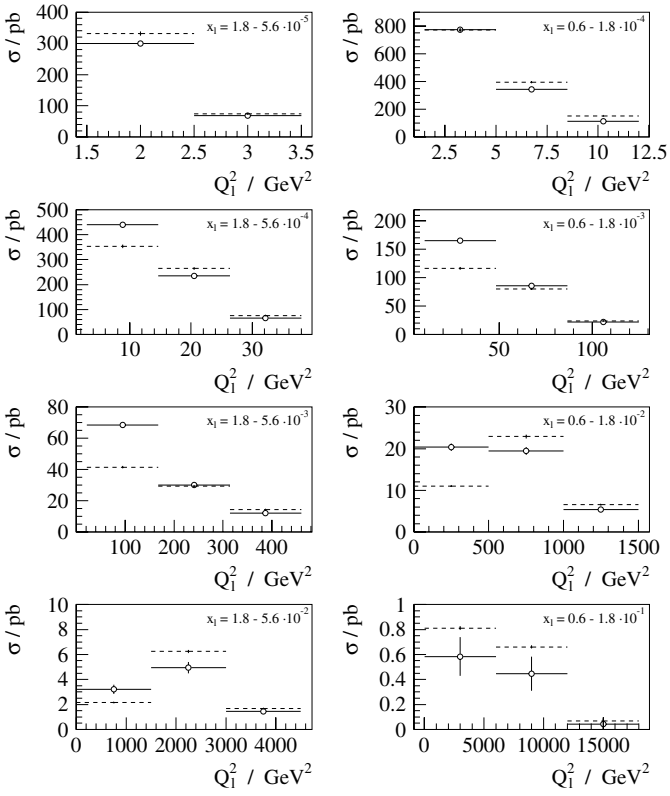

Fig. 7. Double differential cross section of the QED Compton scattering. Open circles depict cross section values given by the COMPTON generator. The corresponding error bars show statistical errors. The dashed lines denote the values computed by Vogelsang

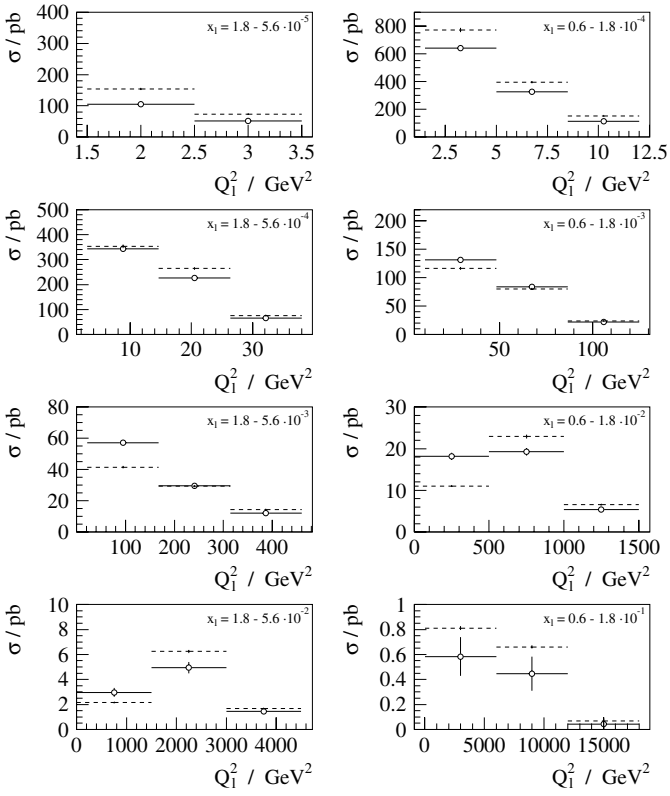

Fig. 8. QED Compton scattering cross section after additional kinematic cuts. Open circles depict cross section values given by the COMPTON generator. The corresponding error bars show statistical errors. The dashed lines show the values computed by Vogelsang

other. This shows, that apparently the equivalent photon approximation does not provide a sufficient degree of accuracy in the inelastic region and that the factorisation of the cross section given by (4) in terms of only two kinematic variables is a too rough approximation of the QEDC scattering process.

In order to ensure the validity of the collinear approximation, additional selection cuts were proposed in [17]:

$$-\hat{t}\,,\hat{s} > 1\,\mathrm{GeV}^2 \qquad \text{and} \qquad p_{t,e}\,,p_{t,\gamma} > 1\,\mathrm{GeV}\ , \quad (5)$$

where the momentum scales $\hat{t}$ and $\hat{s}$ represent the virtualities of the exchanged lepton in the Feynman diagrams shown in Fig. 1. Here, the cuts applied on the transverse momenta $p_{t,e}$ and $p_{t,\gamma}$, actually, have a much stronger effect on the distributions of COMPTON events than those imposed on $\hat{t}$ and $\hat{s}$. After applying all of the four additional cuts the COMPTON QEDC cross section is again compared to the corresponding analytical calculations provided by Vogelsang. As shown in Fig. 8 there are, as before, significant discrepancies observed.

Figure 8 illustrates the difficulties of the collinear approximation. For $Q_l^2 < 5\,\mathrm{GeV}^2$ and $5.6 \cdot 10^{-5} < x_l < 1.8 \cdot 10^{-3}$ the cross sections predictions from the COMPTON program drop significantly when applying the additional cuts on $\hat{t}$, $\hat{s}$ and $p_{t,e}$, $p_{t,\gamma}$. This is not the case for the equivalent photon approximation where the cross sections remain unchanged due to an incorrect calculation of the event kinematics arising from the asumption $p_{t,\gamma^*} = 0$.

It is not ruled out that some carefully chosen cuts on the transverse momenta, polar angles and other event quantities may limit the phase space such that the equivalent photon approximation becomes applicable also for inelastic QEDC scattering. However, with such limitations it is questionable whether the γ function describes a characteristic and universal property of the proton relevant for precision measurements.

5 Concluding remarks

The presented analysis shows that QEDC scattering data at HERA provide the potential to measure the proton structure function F_2 at low Q^2 and medium to high x, extending the kinematic range covered so far into the fixed target region. As such a measurement requires a good understanding of the hadronic final state at low invariant masses, an improved version of the COMPTON generator was developed which allows for a better event modelling.

different start scales Q_0^2 for the integration over F_2, as specified in [17] and (1) of [16]. The differences in γ are in any case of the order of a few percent

With this generator the accuracy of calculations using the equivalent photon approximation is studied. It is revealed that this approximation is not able to describe the inelastic QEDC cross section with sufficient precision. A measurement of the photon density of the proton from QEDC events would, thus, not provide any decisive insight into the proton structure.

Acknowledgements. We would like to thank W. Vogelsang for the fruitful cooperation in the study of the collinear approximation. We are grateful to the H1 collaboration for providing the H1 simulation and reconstruction programs. This work was supported by the Federal Ministry for Education, Science, Research and Technology, FRG, under contract number 05 H1 1PEA/6.

References

1. D. J. Fox et al., Phys. Rev. Lett. **33**, 1504 (1974)
2. J. G. de Groot et al., Z. Phys. C **1**, 143 (1979)
3. C. Adloff et al. [H1 Collaboration], Eur. Phys. J. C **21**, 33 (2001)
4. S. Aid et al. [H1 Collaboration], Nucl. Phys. B **470**, 3 (1996)
5. S. Chekanov et al. [ZEUS Collaboration], Eur. Phys. J. C **21**, 443 (2001)
6. C. Adloff et al. [H1 Collaboration], Phys. Lett. B **393**, 452 (1997)
7. C. Adloff et al. [H1 Collaboration], Nucl. Phys. B **497**, 3 (1997)
8. J. Breitweg et al. [ZEUS Collaboration], Phys. Lett. B **487**, 53 (2000)
9. P. D. Collins, *An Introduction To Regge Theory And High-Energy Physics*, Cambridge, 1977
10. M. Derrick et al. [ZEUS Collaboration], Z. Phys. C **69**, 607 (1996)
11. ZEUS Collaboration, contributed paper to International Conference on High Energy Physics, ICHEP 2002, Amsterdam, abstract **771**
12. H1 Collaboration, contributed paper to International Conference on High Energy Physics, ICHEP 2002, Amsterdam, abstract **976**
13. V. Lendermann, Doctoral Thesis, University of Dortmund, 2002 [DESY–THESIS–02–004].
    The COMPTON program can be obtained from:
    www.physik.uni-dortmund.de/e5/h1/projekte/compton/
14. T. Carli, A. Courau, S. Kermiche and P. Kessler, in *Proceedings of the Workshop "Physics at HERA", Hamburg, 1991*, DESY, 1992, Vol. 2, p. 902 and Vol. 3, p. 1468
15. J. Blümlein, G. Levman and H. Spiesberger, in *Snowmass 1990, Proceedings, Research directions for the decade*, p. 554
16. J. Blümlein, G. Levman and H. Spiesberger, J. Phys. G **19**, 1695 (1993)
17. A. De Rújula and W. Vogelsang, Phys. Lett. B **451**, 437 (1999)
18. A. Courau and P. Kessler, Phys. Rev. D **46**, 117 (1992)
19. T. Ahmed et al. [H1 Collaboration], Z. Phys. C **66**, 529 (1995)
20. F. W. Brasse et al., Nucl. Phys. B **110**, 413 (1976)
21. H. Abramowicz and A. Levy, DESY–97–251, hep–ph/9712415
22. A. Mücke et al., Comput. Phys. Commun. **124**, 290 (2000)
23. T. Sjöstrand et al., Comput. Phys. Commun. **135**, 238 (2001)
24. I. Abt et al. [H1 Collaboration], Nucl. Instrum. Meth. A **386**, 310 (1997) and 348
25. R. D. Appuhn et al. [H1 SpaCal Group], Nucl. Instrum. Meth. A **374**, 149 (1996), A **382**, 395 (1996) and A **386**, 397 (1997)
26. V. Arkadov, Doctoral Thesis, Humboldt University of Berlin, 2000 [DESY–THESIS–00–046]
27. U. Bassler and G. Bernardi, Nucl. Instrum. Meth. A **361**, 197 (1995)
28. H1 Collaboration, contributed paper to International Europhysics Conference on High Energy Physics, EPS 2001, Budapest, abstract **799**
29. L. W. Whitlow et al., Phys. Lett. B **282**, 475 (1992)
30. M. Arneodo et al. [New Muon Collaboration], Nucl. Phys. B **483**, 3 (1997)
31. M. R. Adams et al. [E665 Collaboration], Phys. Rev. D **54**, 3006 (1996)
32. A. Stellberger et al., DESY–03–058, physics/0305070.
33. C. F. von Weizsäcker, Z. Phys. **88**, 612 (1934)
34. E. J. Williams, Phys. Rev. **45**, 729 (1934)
35. J. Blümlein, Z. Phys. C **47**, 89 (1990)
36. M. Drees, R. M. Godbole, M. Nowakowski and S. D. Rindani, Phys. Rev. D **50**, 2335 (1994)
37. J. Ohnemus, T. F. Walsh and P. M. Zerwas, Phys. Lett. B **328**, 369 (1994)
38. J. Ohnemus, S. Rudaz, T. F. Walsh and P. M. Zerwas, Phys. Lett. B **334**, 203 (1994)
39. M. Glück, M. Stratmann and W. Vogelsang, Phys. Lett. B **343**, 399 (1995)
40. M. Glück, C. Pisano and E. Reya, Phys. Lett. B **540**, 75 (2002)
41. M. Glück, C. Pisano, E. Reya and I. Schienbein, Eur. Phys. J. C **27**, 427 (2003)
42. H. Anlauf et al., DESY–91–018
43. W. Vogelsang (private communication)